ISSN 1070-3284, Russian Journal of Coordination Chemistry, 2024, Vol. 50, No. 6, pp. 405–414. © Pleiades Publishing, Ltd., 2024.

Coordination Compounds of Alkali and Rare Earth Metals Based on Centrosymmetric Chlorine-Substituted Bismercaptooxazole. Synthesis, Structure, and Luminescence

A. F. Rogozhin[a], *, V. A. Ilichev[a], L. I. Silantyeva[a], T. A. Kovylina[a], E. A. Kozlova[a], G. K. Fukin[a], and M. N. Bochkarev[a]

[a] *Razuvaev Institute of Organometallic Chemistry, Russian Academy of Sciences, Nizhny Novgorod, Russia*

**e-mail: atonrog@iomc.ras.ru*

Received December 29, 2023; revised January 23, 2024; accepted January 24, 2024

Abstract—New coordination polymers were synthesized. A ditopic centrosymmetric organic ligand containing oxazole heterocycles, 4,8-dichlorobenzo[1,2d:4,5d']bis(oxazole)-2,6(3H,7H)-dithione (H_2L), was prepared and structurally characterized. It was shown that deprotonated H_2L forms non-luminescent binuclear molecular complexes $Li_2L(THF)_6$ (**I**) and $Na_2L(DME)_4$ (**II**) with alkali metals, while complexes of H_2L with lanthanides are ionic compounds $[Ln(DMSO)_8][L]_{1.5}$ (Ln = Nd (**III**), Yb (**IV**)) exhibiting moderate metal-centered emission in the near-infrared (IR) range, despite the absence of coordination of the ligand L to lanthanide ions. The molecular structures of $H_2L{\cdot}2DMSO$ and **I**–**III** were established by X-ray diffraction (CCDC nos. 2320461 ($H_2L{\cdot}2DMSO$), 2320462 (**I**), 2320463 (**II**), 2320464 (**III**)).

Key words: lanthanides, benzoxazole, photoluminescence, alkali metals, heterocyclic ligands

DOI: 10.1134/S1070328424600177

INTRODUCTION

Lanthanide-based coordination polymers (CPs) attract attention owing to some unique features. First of all, the photoluminescence (PL) of lanthanide ions, which has narrow emission bands both in the visible and near-infrared spectral ranges [1–3], can be significantly enhanced by organic linkers acting as antennas, which efficiently absorb and transfer the excitation energy to the metal. These compounds can be used as luminophores with metal-centered emission of lanthanide ions [4–6], fluorescent sensors [7–9], magnets [10, 11], scintillators [12], heterogeneous catalysts [13], and for some other applications [14–16]. Among the diversity of polytopic linkers capable of forming CPs, the use of carboxylic acid [17–19] and imidazole derivatives [20, 21], which are hard Lewis acids, is widely known. Previously, it was demonstrated that soft-base bisthiazolate linkers can also be used for the synthesis of luminescent CPs based on lanthanides and alkali metals [22, 23]. At the time this work was initiated, there were only data on the use of a bismercaptothiazole ditopic linker, benzo[1,2:4,5]-bis(thiazole)-2,6-dithiol, for the formation of luminescent CPs based on lanthanides. A specific feature of this linker is the presence of an inversion center in the molecular structure. In order to expand the range of centrosymmetric soft-base ditopic ligands capable of forming luminescent lanthanide-containing CPs, we decided to shift the focus of attention to ditopic derivatives of 2-mercaptooxazole, particularly, 4,8-dichlorobenzo[1,2d:4,5d']bis(oxazole)-2,6(3H,7H)-di-thione (H_2L). The selection of oxazole heterocycle is caused by the fact that its compounds are efficient sensitizers of Ln^{3+} luminescence [24–27]. In addition, recent studies of chlorine-containing antenna systems showed an increase in the efficiency of IR photoluminescence (PL) for some lanthanides, in particular neodymium [28, 29].

EXPERIMENTAL

All reactions and handling of compounds were carried out using the Schlenk technique or under the atmosphere of an argon glove box ($O_2 < 1$ ppm; $H_2O <$ 0.1 ppm). All reagents and solvents were received from commercial sources. 1,2-Dimethoxyethane (DME), 1,4-dioxane, and tetrahydrofuran (THF) were dried with sodium benzophenone ketyl by the standard procedure and withdrawn in vacuo immediately before use. Dimethyl sulfoxide (DMSO) was dried over 3 Å sieves. 2,5-Diamino-3,6-dichloro-1,4-benzoquinone was synthesized by a known procedure from commercially available 2,3,5,6-tetrachlorocyclohexa-2,5-diene-1,4-dione and aqueous ammonia [30].

The elemental analysis for C, H, N, and S was carried out on a Euro EA 3000 elemental analyzer. Neodymium and ytterbium contents were analyzed by complexometric titration. IR spectra were recorded on a FSM1201 FTIR spectrometer in the range from 4000 to 450 cm^{-1} in mineral oil on KBr substrates. The NMR spectra were recorded on a Bruker Avance III spectrometer (400 MHz) in DMSO-d_6 using Me_4Si as the internal standard. Mass spectra were run on a Polaris Q/Trace GC Ultra gas chromatograph/mass spectrometer with an electron ionization energy of 70 eV in the 40–700 range of mass numbers. The photoluminescence of solid samples was excited by a 100 mW diode laser at 405 nm and recorded in the range from 400 to 1700 nm with OceanOptics USB2000 and OceanOptics NIR 512 spectrofluorimeters.

Synthesis of 4,8-dichlorobenzo[1,2-d:4,5-d']-bis(oxazole)-2,6(3H,7H)-dithione (H_2L). A 50 mL flask was charged with DMSO (15 mL), 2,5-diamino-3,6-dichloro-1,4-benzoquinone (1 g, 4.83 mmol), carbon disulfide (1.5 mL, 24.94 mmol), and sodium sulfide nonahydrate (1.159 g, 4.83 mmol). The mixture was heated at reflux under argon on an oil bath at 100°C with vigorous magnetic stirring for 12 h. The beige solution darkened to a red-brown color. The mixture was cooled to room temperature, an aqueous solution (15 mL) of NaOH (1 g) was added, and the mixture was stirred for 30 min until sulfur precipitated. The precipitated sulfur was filtered off on a glass filter, and 1 M HCl was added until pH was 3–4. The resulting curdy precipitate was filtered off, washed with water, and dried in vacuo at 100°C for 2 h. H_2L was isolated as a gray-brown powder in a yield of 1.26 g (89%). Crystals of $H_2L{\cdot}2DMSO$ were formed on slow cooling of a hot saturated solution of H_2L in DMSO.

^{13}C NMR (δ, ppm): 95.80, 127.87, 142.90, 180.41. IR (ν, cm^{-1}): 466 w, 520 s, 559 w, 572 w, 661 m, 903 m, 922 s, 995 s, 1136 s, 1235 s, 1400 m, 1533 m, 1559 s, 1580 w, 1752 w, 3074 s; MS (M = 292.09).

For $C_8H_2N_2O_2Cl_2S_2$

Anal. calcd., %	C, 32.78	H, 0.69	N, 9.56	S, 21.87
Found, %	C, 32.74	H, 0.68	N, 9.52	S, 21.68

Synthesis of $Li_2L(THF)_6$ (I). A solution of $LiN(SiMe_3)_2$ (0.682 mmol, 109.8 mg) in THF (5 mL) was added to a suspension of H_2L (0.341 mmol, 100 mg) in THF (5 mL) obtained by stirring in an ultrasonic bath, and the reaction mixture was sealed in a tube. The color of the mixture sharply changed to brown. The mixture was stirred in an ultrasonic bath for 10 min. After 24 h, the resulting colorless crystals were decanted, washed with cold hexane, and dried in vacuo at room temperature. The crystalline target product was isolated in a yield of 158 mg (63%). The crystals for X-ray diffraction were taken directly from the reaction tube.

IR (ν, cm^{-1}): 466 m, 503 s, 585 w, 622 w, 646 w, 683 m, 754 m, 823 m, 873 s, 905 s, 995 s, 1048 s, 1258 s, 1339 s, 1496 m, 1580 w, 1620 w, 1922 w.

For $C_{32}H_{48}N_2O_8S_2Cl_2Li_2$

Anal. calcd., %	C, 52.11	H, 6.56	N, 3.80	S, 8.69
Found, %	C, 52.02	H, 6.54	N, 3.79	S, 8.51

The synthesis of $Na_2L(DME)_4$ (II) was carried out by a procedure similar to that described for **I** by dissolving H_2L (0.341 mmol, 100 mg) and $NaN(SiMe_3)_2$ (0.682 mmol, 123.6 mg). The color of the solution changed to green. The target product was isolated as colorless crystals in a yield of 171.3 mg (72%). The crystals for X-ray diffraction were taken directly from the reaction tube.

IR (ν, cm^{-1}): 500 m, 572 m, 683 w, 805 w, 820 w, 863 s, 900 w, 992 s, 1019 w, 1032 w, 1061 m, 1090 s, 1125 w, 1196 m, 1260 m, 1278 w, 1326 m, 1599 m, 1911 w, 1951 w.

For $C_{24}H_{40}N_2O_{10}S_2Cl_2Na_2$

Anal. calcd., %	C, 41.32	H, 5.78	N, 4.02	S, 9.19
Found, %	C, 41.27	H, 5.76	N, 4.01	S, 9.04

Synthesis of $[Nd(DMSO)_8][L]_{1.5}$ (III). A solution of $Nd[N(SiMe_3)_2]_3$ (0.227 mmol, 142.2 mg) in THF (5 mL) was added to a suspension of H_2L (0.341 mmol, 100 mg) in THF (5 mL) obtained by stirring in an ultrasonic bath. The color of the reaction mixture sharply changed to dark green. The reaction mixture was stirred in an ultrasonic bath for 10 min. The solvent and volatile products were removed in vacuo. A DMSO : dioxane mixture in 1 : 3 ratio was added to the dried precipitate. Then the sealed reaction tube was kept for 48 h at 60°C. The resulting light blue crystals were collected on a filter, washed with cold hexane, and dried in vacuo at room temperature. Complex **III** was isolated in a yield of 115 mg (42%). The crystals for X-ray diffraction were taken directly from the reaction tube.

IR (ν, cm^{-1}): 466 w, 498 s, 569 w, 614 w, 683 m, 823 s, 897 m, 955 s, 1006 s, 1045 s, 1098 w, 1212 w, 1249 s, 1318 m, 1534 w, 1665 m, 1909 m, 2054 m, 3418 m.

For $C_{28}H_{48}N_3O_{11}S_{11}Cl_3Nd$

Anal. calcd., %	C, 27.89	H, 4.01	N, 3.48	S, 29.24	Nd, 11.96
Found, %	C, 27.85	H, 3.98	N, 3.47	S, 29.01	Nd, 12.03

Synthesis of $[Yb(DMSO)_8][L]_{1.5}$ (IV). Complex **IV** was synthesized similarly to complex **III** using H_2L (0.341 mmol, 100 mg) and $Yb[N(SiMe_3)_2]_3$ (0.227 mmol, 148.7 mg). After drying, the color of the

Table 1. Crystallographic characteristics and X-ray experiment and structure refinement details of complexes H_2L·2DMSO, **I**–**III**

Parameter	Value			
	H_2L·2DMSO	**I**	**II**	**III**
Molecular formula	$C_{12}H_{14}N_2O_4S_4Cl_2$	$C_{32}H_{48}N_2OS_2Cl_2Li_{28}$	$C_{24}H_{40}Cl_2N_2Na_2O_{10}S_2$	$C_{28}H_{48}C_{l3}N_3NdO_{11}S_{11}$
M, g/mol	449.39	737.62	697.58	1205.94
Temperature, K	100(2)	100(2)	100(2)	100(2)
System	Monoclinic	Monoclinic	Monoclinic	Monoclinic
Space group	$C2/c$	$P2_1/n$	$P2_1/n$	$P2_1/n$
a, Å	21.9776(9)	8.8269(3)	8.6939(4)	12.7512(2)
b, Å	9.5988(4)	13.4479(3)	13.8784(7)	24.4450(4)
c, Å	17.6818(9)	15.8333(4)	14.1773(7)	15.7342(3)
β, deg	90.072(4)	104.022(3)	99.696(5)	95.4732(17)
V, Å^3	3730.1(3)	1823.46(9)	1686.16(14)	4882.04(15)
Z	8	2	2	4
ρ(calcd.), g/cm^3	1.600	1.343	1.374	1.641
μ, mm^{-1}	0.815	0.342	0.393	1.750
F(000)	1840	780	732	2448
Crystal size	0.60 × 0.29 × 0.18	0.42 × 0.17 × 0.06	0.43 × 0.33 × 0.19	0.35 × 0.25 × 0.09
θ, deg	2.304–30.033	2.013–29.130	2.068–28.000	1.966–27.103
Number of reflections: measured/unique	42145/5454	30716/4893	38068/4076	86943/10772
R_{int}	0.0548	0.0713	0.1147	0.0722
R_1/wR_2 (all reflections)	$R_1 = 0.0564$, $wR_2 = 0.1025$	$R_1 = 0.0776$, $wR_2 = 0.1202$	$R_1 = 0.0596$, $wR_2 = 0.1265$	$R_1 = 0.0572$, $wR_2 = 0.0705$
R_1/wR_2 ($I > 2\sigma(I)$)	$R_1 = 0.0399$, $wR_2 = 0.0938$	$R_1 = 0.0458$, $wR_2 = 0.1038$	$R_1 = 0.0455$, $wR_2 = 0.1166$	$R_1 = 0.0342$, $wR_2 = 0.0631$
S(F^2)	1.081	1.044	1.049	1.024
$\Delta\rho_{min}/\Delta\rho_{max}$, e/Å^3	0.789/–0.729	0.387/–0.306	0.412/–0.375	0.962/–0.795

reaction mixture changed to dark brown. Complex **IV** was isolated as a finely crystalline yellow-orange powder in a yield of 109.3 mg (39%). The IR spectrum of **IV** was similar to that of **III**.

For $C_{28}H_{48}N_3O_{11}S_{11}Cl_3Yb$

Anal calcd., %	C, 27.24	H, 3.92	N, 3.40	S, 28.56	Yb, 14.02
Found, %	C, 27.17	H, 3.89	N, 3.39	S, 28.17	Yb, 14.17

X-ray diffraction study of compounds H_2L·2DMSO, **I**–**III** was carried out on an Oxford Xcalibur Eos diffractometer (graphite monochromator, MoK_α radiation, ω-scan mode, λ = 0.71073 Å). The experimental sets of intensities were integrated using the CrysAlisPro program [31]. The absorption corrections were applied using the SCALE3 ABSPACK scaling algorithm implemented in the CrysAlisPro software. The structures were solved by the SHELXT program [32] and refined by the full-matrix least-squares method on F^2_{hkl} in the anisotropic approximation for all non-hydrogen atoms by the SHELXL program [33]. All hydrogen atoms of H_2L, except for H(1A) and H(2A), were placed into geometrically calculated positions and refined in the isotropic approximation in the riding model: $U_{iso}(H) = 1.5\ U_{eq}(C)$ for methyl groups and $U_{iso}(H) = 1.2\ U_{eq}(C)$ for all other groups. In turn, the H1A and H2A atoms in H_2L were located objectively from the difference Fourier maps and refined in the isotropic approximation. Fragments of the coordinated solvent molecules in complexes **I** (THF), **II** (DME), and **III** (DMSO) are disordered over two positions. The refinement was performed using ISOR, EADP, SADI, and DFIX instructions. The main crystallographic characteristics of compounds H_2L·2DMSO (**I**–**III**) are summarized in Table 1.

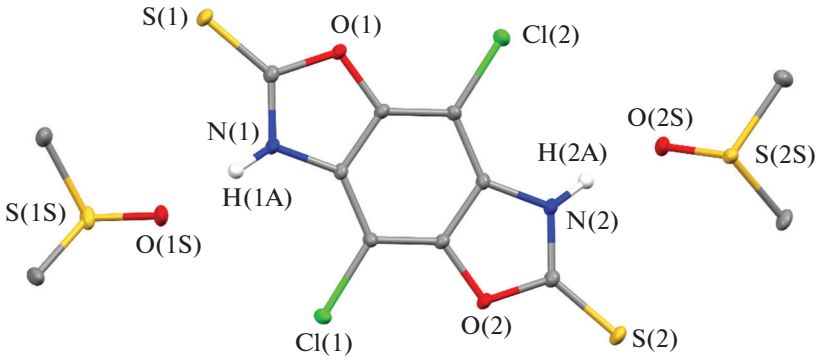

Fig. 1. Molecular structure of $H_2L{\cdot}2DMSO$. Ellipsoids are given at 30% probability. The hydrogen atoms of DMSO are omitted for clarity.

The structures were deposited with the Cambridge Crystallographic Data Centre (CCDC nos. 2320461 ($H_2L{\cdot}2DMSO$), 2320462 (**I**), 2320463 (**II**), 2320464 (**III**); deposit@ccdc.cam.ac.uk or http://www.ccdc.cam.ac.uk/).

RESULTS AND DISCUSSION

The synthesis of the target bismercaptooxazole H_2L was performed in two steps (Scheme 1). In the first step, commercially available 2,3,5,6-tetrachlorocyclohexa-2,5-diene-1,4-dione was converted to 2,5-diamino-3,6-dichloro-1,4-benzoquinone by the nucleophilic substitution reaction with aqueous ammonia [30]. Then the resulting benzoquinone was condensed with carbon disulfide in DMSO in the presence of sodium sulfide nonahydrate, which acted as a reducing agent for benzoquinone. The target compound was isolated as a gray powder in 89% yield and characterized by IR and ^{13}C NMR spectroscopy, mass spectrometry, and elemental analysis. The resulting bismercaptooxazole is stable in air; soluble in highly alkaline aqueous media; insoluble in water, toluene, hexane, acetonitrile, and diethyl ether; and sparingly soluble in DME, THF, and DMSO.

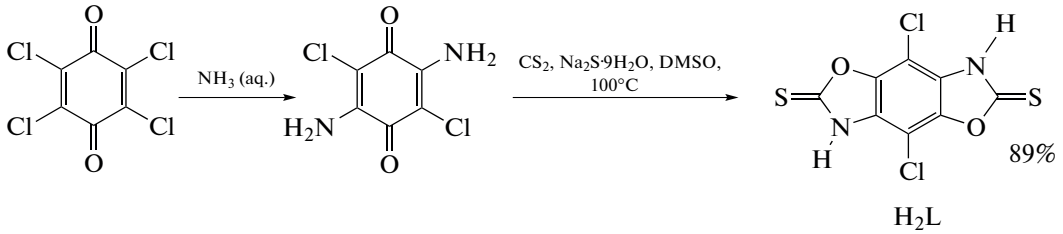

Scheme 1. Synthesis of ditopic ligand H_2L.

Slow cooling of a hot saturated solution of H_2L in DMSO gave crystals of the H_2L adduct with two DMSO molecules, suitable for X-ray diffraction.

The molecular structure of the obtained bismercaptooxazole is shown in Fig. 1. The N–H hydrogen atoms are oriented towards the oxygen atoms of two DMSO molecules: The H...O hydrogen bond lengths are 1.76(3) and 1.78(3) Å. The bismercaptooxazole molecule is virtually planar. The maximum deviation of non-hydrogen atoms was 0.025 Å. The bond length distribution in the H_2L molecule is in good agreement with these values for related compounds (Tables 2 and 3) [34, 35].

In the crystal packing, bismercaptooxazole molecules form one-dimensional stacks (Fig. 2). The dihedral angles between the planes of neighboring H_2L molecules are 0° and 8.8°, and the distances between the center of the aromatic ring of one molecule and the middle of the C=S bond of another molecule are 3.73 and 3.55 Å, respectively. These geometric characteristics attest to the intermolecular π...π interaction in the crystal [36].

In order to synthesize CPs based on alkali metal ions, the reactions of sodium and lithium silylamide complexes with H_2L were performed as shown in Scheme 2. However, X-ray diffraction data indicate that the colorless crystals of compounds **I** and **II** formed in these reactions are binuclear molecular complexes $M_2L(solv)_n$, where M = Li, Na, solv = THF ($n = 6$), DME ($n = 4$).

Table 2. Selected bond lengths (Å) of complexes $H_2L{\cdot}2DMSO$, **I**–**III**

Bond	Length, Å	Bond	Length, Å
$H_2L{\cdot}2DMSO$		**I**	
Cl(1)C(3)	1.716(2)	Li(1)O(2)	1.944(4)
Cl(2)C(7)	1.709(2)	Li(1)O(3)	1.974(4)
S(1)C(1)	1.645(2)	Li(1)O(4)	1.962(4)
S(2)C(5)	1.644(2)	Li(1)N(1)	2.077(4)
O(1)C(1)	1.382(2)		
O(1)C(8)	1.374(2)		
O(2)C(4)	1.373(2)		
O(2)C(5)	1.382(2)		
N(1)C(1)	1.347(3)		
N(1)C(2)	1.385(2)		
N(1)H(1A)	0.87(3)		
N(2)C(5)	1.346(3)		
N(2)C(6)	1.389(2)		
N(2)H(2A)	0.91(3)		
II		**III**	
Na(1)O(2)	2.3700(16)	Nd(1)O(1)	2.486(2)
Na(1)O(3)	2.382(2)	Nd(1)O(2)	2.399(2)
Na(1)O(3A)	2.38(2)	Nd(1)O(3)	2.389(2)
Na(1)O(4)	2.3532(16)	Nd(1)O(3)	2.389(2)
Na(1)O(5)	2.4131(15)	Nd(1)O(6)	2.486(2)
Na(1)N(1)	2.3639(17)	Nd(1)O(7)	2.434(2)
Na(1)S(1)	3.0648(10)	Nd(1)O(8)	2.465(2)

$$2MN(Si(Me)_3)_2 + H_2L \xrightarrow{solv.} M_2L(solv)_n$$

I: M = Li, solv = THF, n = 6, 76%

II: M = Na, solv = DME, n = 4, 84%

Scheme 2. Synthesis of binuclear alkali metal complexes **I** and **II**.

Compound **I** is a binuclear lithium complex in which each metal atom is bound to one nitrogen atom of bismercaptooxazole and to three THF molecules (Fig. 3). The Li(1)–N(1) bond length is 2.077(4) Å. The ligand coordination results in some elongation of the C=S bond (1.673(2) Å) compared to that in the free ligand (1.645(2) Å); however, the Li...S distance (3.392(4) Å) is much longer than the sum of the lithium ionic radius (0.73 Å) [37] and van der Waals radius of sulfur (1.8 Å) [38], indicating the absence of the Li...S interaction. Thus, the lithium coordination environment is a distorted tetrahedron. The main geometric characteristics of the lithium coordination sphere (Tables 2 and 3) are in line with the values observed in previously reported related complexes [39]. Bismercaptooxazole in complex **I** has a planar structure. The maximum deviation from the plane is 0.033 Å.

Compound **II**, like **I**, is a binuclear complex (Fig. 4). Each sodium atom is bound to two DME molecules and to the nitrogen and sulfur atoms of the bismercaptooxazole ligand. The Na(1)–S(1) distance is 3.0648(10) Å, which is only slightly greater than the sum of the sodium ionic radius (1.16 Å) [37] and the van der Waals radius of sulfur (1.8 Å) [34]. In general, the main geometric characteristics in the sodium coordination sphere of **II** (Tables 2 and 3) are in good agreement with those for previously reported six-coordinate sodium compounds with related ligands [23]. Note that the C=S distance in complex **II** (1.685(2)) increases relative to that in **I** (1.673(2) Å), which is indicative of the presence of Na...S interaction (3.0648(10)) [40]. The coordination sphere of sodium is a distorted octahedron. As in complex **I**, bis-mercaptooxazole is planar. The maximum deviation from the plane is 0.012 Å.

In order to synthesize lanthanide-containing CPs based on ditopic bis-mercaptooxazole H_2L, reactions of neodymium and ytterbium silylamide complexes $Ln[N(Si(Me)_3)_2]_3$ with free bisthiazole were carried out in three steps in accordance with Scheme 3. After heating for 2 days at a temperature of 60°C, in the case of neodymium, light blue crystals of compound **III** were found. According to X-ray diffraction data, this was the ionic complex $[Nd(DMSO)_8][L]_{1.5}$.

$$Ln[N(Si(Me)_3)_2]_3 + 1.5H_2L \xrightarrow[(2)\ -THF,\ 3\ HN(Si(Me)_3)_2]{(1)\ +THF,\ Ultrasonication} [Ln(DMSO)_8][L]_{1.5}$$
$$(3)\ DMSO : Dioxane\ 1 : 3,\ 60°C$$

III: Ln = Nd, 67%

IV: Ln = Yb, 59%

Scheme 3. Synthesis of ionic compounds of lanthanides **III** and **IV**.

According to X-ray diffraction data, complex **III** was structurally similar to the previously reported neodymium complex with a related bisthiazole ligand [22]. Complex **III** was composed of the cationic $Nd^{3+}(DMSO)_8$ and anionic L^{2-} parts, with three bis-mercaptooxazole dianions per two cationic parts being present in the crystal. The molecular structure of complex **III** is shown in Fig. 5.

The Nd–O distances vary over a broad range from 2.389(2) to 2.486(2) Å (Table 2). The coordination

Table 3. Selected angles (deg) in complexes $H_2L{\cdot}2DMSO$, **I**–**III**

Angle	ω, deg	Angle	ω, deg
$H_2L{\cdot}2DMSO$		**I**	
C(8)O(1)C(1)	107.51(15)	O(2)Li(1)O(4)	113.02(18)
C(4)O(2)C(5)	107.30(15)	O(2)Li(1)O(3)	99.69(17)
C(1)N(1)C(2)	109.72(17)	O(4)Li(1)O(3)	96.40(16)
C(1)N(1)H(1A)	122.8(19)	O(2)Li(1)N(1)	100.03(17)
C(2)N(1)H(1A)	127.2(19)	O(4)Li(1)N(1)	114.07(18)
C(5)N(2)C(6)	109.51(17)	O(3)Li(1)N(1)	132.93(19)
C(5)N(2)H(2A)	124.2(18)		
C(6)N(2)H(2A)	125.1(18)		
N(1)C(1)O(1)	108.17(16)		
N(1)C(1)S(1)	130.15(16)		
O(1)C(1)S(1)	121.67(15)		
N(1)C(2)C(8)	105.96(17)		
N(1)C(2)C(3)	132.80(18)		
II		**III**	
O(4)Na(1)N(1)	116.07(6)	O(3)Nd(1)O(2)	92.82(9)
O(4)Na(1)O(2)	91.91(6)	O(3)Nd(1)O(4)	86.63(9)
N(1)Na(1)O(2)	95.92(6)	O(2)Nd(1)O(4)	139.88(8)
O(4)Na(1)O(3A)	105.4(5)	O(3)Nd(1)O(5)	149.66(8)
N(1)Na(1)O(3A)	136.3(5)	O(2)Nd(1)O(5)	86.21(8)
O(2)Na(1)O(3A)	68.7(2)	O(4)Nd(1)O(5)	75.16(8)
O(4)Na(1)O(3)	91.21(8)	O(3)Nd(1)O(7)	92.70(9)
N(1)Na(1)O(3)	150.27(8)	O(2)Nd(1)O(7)	150.80(8)
O(2)Na(1)O(3)	70.17(6)	O(4)Nd(1)O(7)	69.09(8)
O(4)Na(1)O(5)	71.15(5)	O(5)Nd(1)O(7)	102.84(9)
N(1)Na(1)O(5)	93.78(6)	O(3)Nd(1)O(8)	137.53(8)
O(2)Na(1)O(5)	162.90(7)	O(2)Nd(1)O(8)	75.42(8)
O(3A)Na(1)O(5)	112.7(3)	O(4)Nd(1)O(8)	128.31(8)
O(3)Na(1)O(5)	106.83(6)	O(5)Nd(1)O(8)	71.40(8)
O(4)Na(1)C(1)	141.23(6)	O(7)Nd(1)O(8)	81.24(8)
N(1)Na(1)C(1)	25.81(5)	O(3)Nd(1)O(6)	70.05(8)
O(2)Na(1)C(1)	97.86(6)	O(2)Nd(1)O(6)	82.13(9)
O(3A)Na(1)C(1)	113.1(5)	O(4)Nd(1)O(6)	133.99(9)
O(3)Na(1)C(1)	127.41(8)	O(5)Nd(1)O(6)	139.35(8)
O(5)Na(1)C(1)	97.01(5)	O(7)Nd(1)O(6)	72.92(9)
O(4)Na(1)S(1)	166.82(5)	O(8)Nd(1)O(6)	67.99(7)
N(1)Na(1)S(1)	58.22(4)	O(3)Nd(1)O(1)	74.30(8)
O(2)Na(1)S(1)	100.36(5)	O(2)Nd(1)O(1)	71.58(7)
O(3A)Na(1)S(1)	83.7(5)	O(4)Nd(1)O(1)	69.71(8)
O(3)Na(1)S(1)	97.43(7)	O(5)Nd(1)O(1)	76.66(8)
O(5)Na(1)S(1)	96.72(4)	O(7)Nd(1)O(1)	137.34(8)
C(1)Na(1)S(1)	32.46(4)	O(8)Nd(1)O(1)	135.00(8)
		O(6)Nd(1)O(1)	134.08(8)

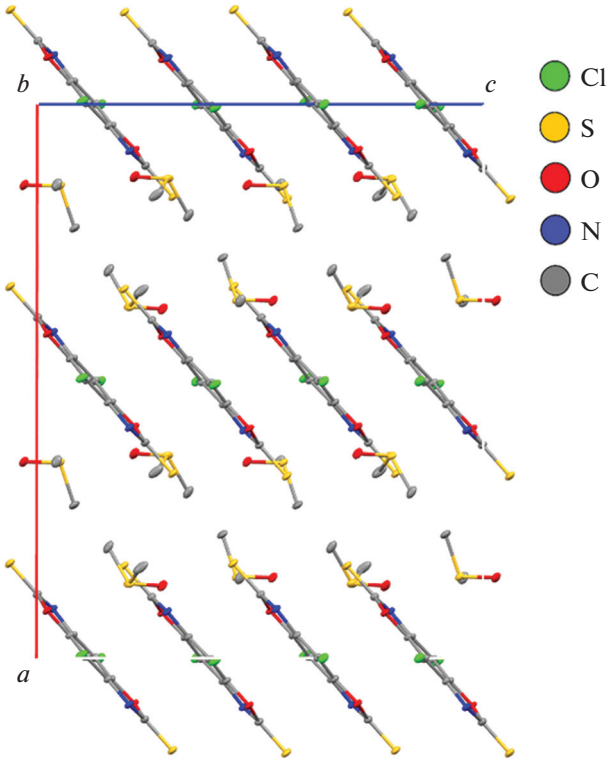

Fig. 2. Fragment of the crystal packing of H_2L complex. The crystallographic projection along the *b* axis is presented. The hydrogen atoms are omitted for clarity.

sphere of neodymium in **III** is a distorted square antiprism. The bismercaptooxazole dianions have a planar structure. The greatest deviations from the plane are 0.047 and 0.127 Å. The main geometric characteristics are in good agreement with those for previously reported Nd(III) complex [22]. The main difference between complex **III** and the related bisthiazole complex [22] is in the mutual arrangement of the anionic moieties relative to each other. Whereas in the previously described complex, the planes of neighboring ligands form a dihedral angle of 58.8°, in complex **III**, these planes are nearly perpendicular (81.3°). In addition, the distance between the chlorine atom of one ligand to the center of the aromatic ring of the other ligand is 3.375 Å (Fig. 6), indicating the presence of C–Cl...π interactions in the crystal of **III** [41].

For ytterbium-containing product **IV**, crystals suitable for X-ray diffraction could not be obtained; however, the similarity of the elemental composition and IR spectra of **IV** and **III** provides the conclusion that its structure is identical to that of neodymium compound **III**.

It was found that the molecular binuclear lithium and sodium complexes based on the chloride-containing ditopic bismercaptooxazole H_2L (**I** and **II**) were not luminescent at either room or liquid nitrogen temperatures, while related 2-mercaptobenzoxazole [42] was found to exhibit luminescence.

Despite the absence of PL in alkali metal salts, compounds **III** and **IV** exhibited metal-centered PL of moderate intensity in the near-IR region caused by the corresponding lanthanide ions, despite the absence of coordination of bismercaptooxazole to the metal atoms. The PL spectra (Fig. 7) of compounds **III** and **IV** recorded upon excitation with a diode laser at 405 nm show the emission bands with intraconfigurational *f*–*f* transitions characteristic of the corresponding lanthanide ions: Nd, $^4F_{3/2} \rightarrow {}^4I_{9/2}$ (855 nm); $^4F_{3/2} \rightarrow {}^4I_{11/2}$ (1055 nm) and $^4F_{3/2} \rightarrow {}^4I_{13/2}$ (1345 nm); Yb, $^4F_{3/2} \rightarrow {}^4I_{9/2}$ (990 nm). Hence, deprotonated H_2L ligand acts as a sensitizer of lanthanide luminescence.

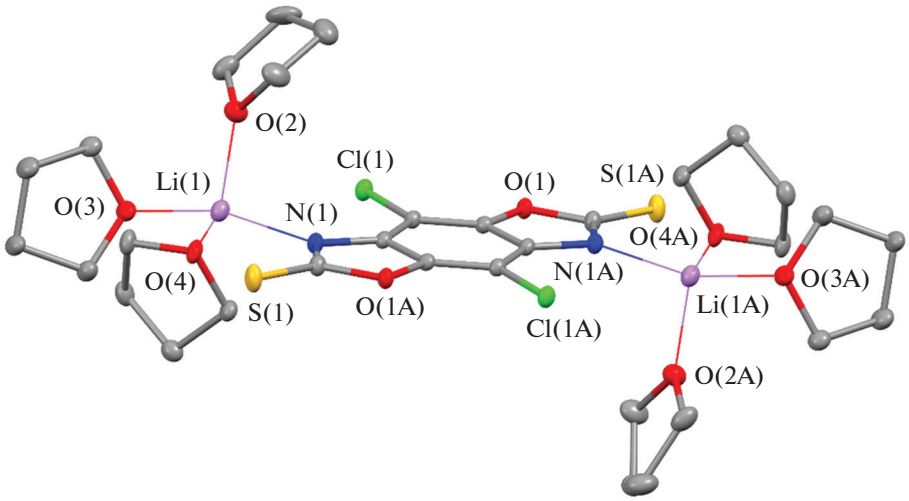

Fig. 3. Molecular structure of complex **I**. Ellipsoids are given at 30% probability. The hydrogen atoms are omitted for clarity. Symmetry code used to generate equivalent atoms (A): $1/2 - x$, $1/2 + y$, $1/2 - z$.

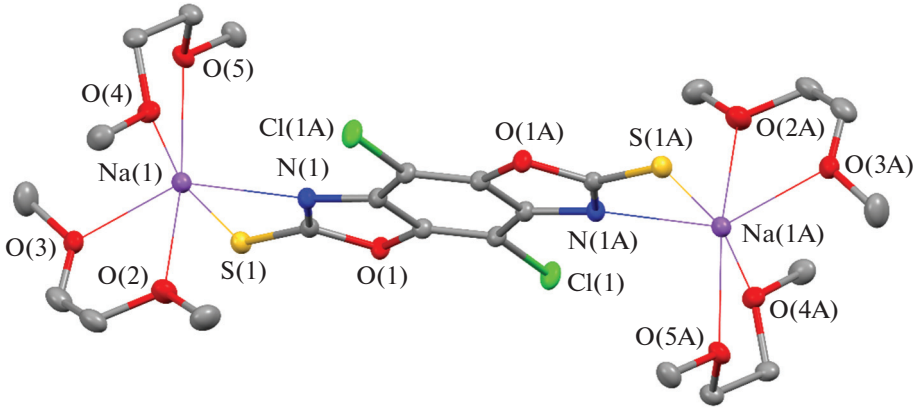

Fig. 4. Molecular structure of complex **II**. Ellipsoids are given at 30% probability. The hydrogen atoms are omitted for clarity. Symmetry code used to generate equivalent atoms (A): $1/2 - x$, $1/2 + y$, $1/2 - z$.

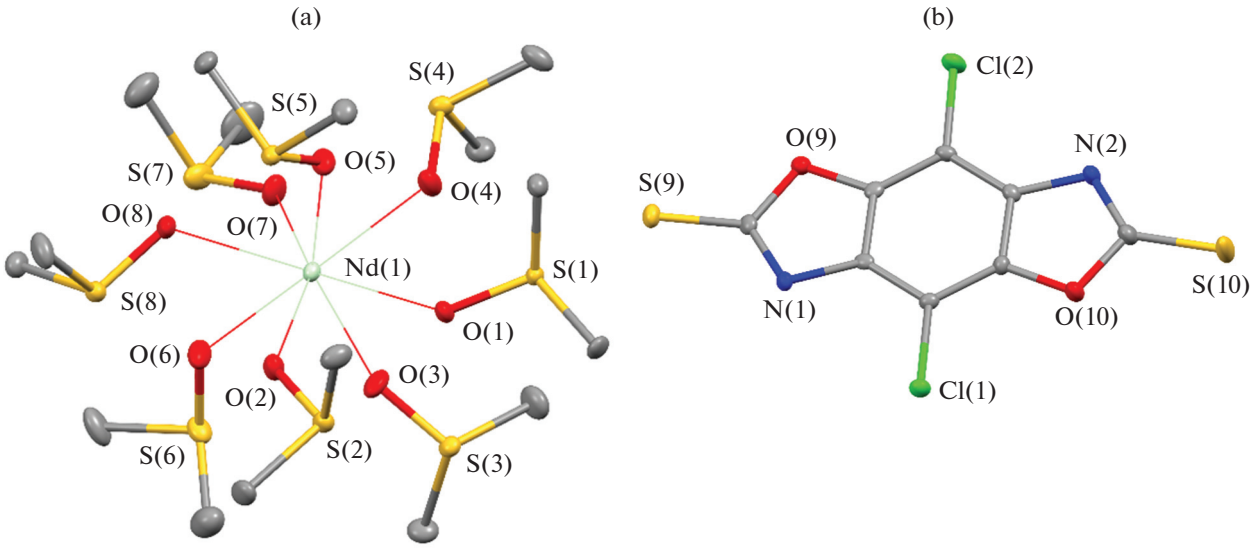

Fig. 5. (a) Cationic and (b) anionic parts of complex **III**. Ellipsoids are given at 30% probability. The hydrogen atoms are omitted for clarity.

Attempts to synthesize lanthanide-containing coordination polymers using methods successfully applied to related bismercaptothiazole ditopic linkers [22] were unsuccessful in the case of H_2L. Probably, this is attributable to the fact that its molecule contains relative large substituents, chlorine atoms, which prevent the formation of 2D layers, and to the additional stabilization of ionic salts by C–Cl...π interactions in the crystals.

Thus, a new ditopic centrosymmetric heterocyclic ligand containing two annulated oxazole heterocycles, 4,8-dichlorobenzo[1,2-d:4,5-d']bis(oxazole)-2,6(3H,7H)-dithione (H_2L), was synthesized and structurally characterized. It was shown that dilithium and disodium salts of this compound, $Li_2L(THF)_6$ and $Na_2L(DME)_4$, are non-luminescent molecular complexes in which sodium atoms are chelated by the S^N moiety, while lithium is coordinated only to nitrogen. With neodymium and ytterbium ions, deprotonated H_2L forms ionic compounds $[Ln(DMSO)_8][L]_{1.5}$, which show moderate PL characteristic of these atoms in the near-IR region.

ACKNOWLEDGMENTS

This study was performed using the research equipment of the Center for Collective Use "Analytical Center of the Razuvaev Institute of Organometallic Chemistry, Russian Academy of Sciences," supported by the grant "Provision of the Development of Material and Technical Infrastructure of Centers for the Collective Use of Research Equipment" (unique identifier RF–2296.61321X0017, agreement no. 075-15-2021-670).

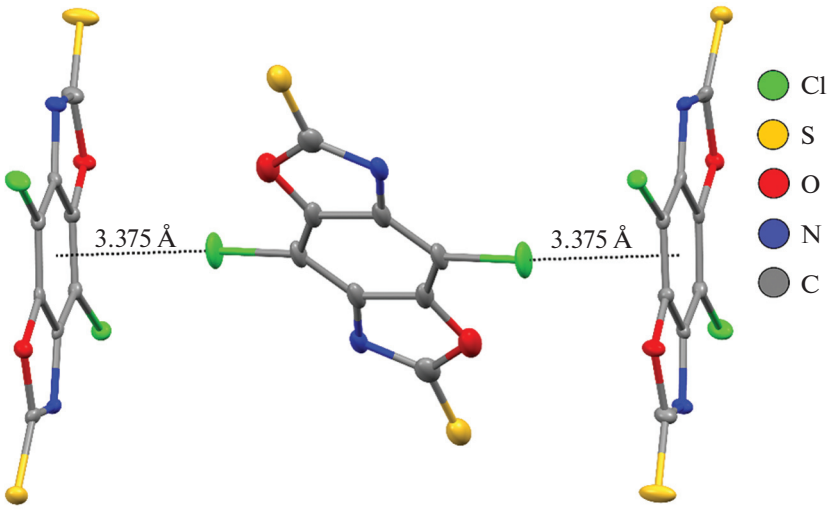

Fig. 6. Arrangement of the bismercaptooxazole dianions in complex **III**. Ellipsoids are given at 30% probability. The hydrogen atoms are omitted for clarity.

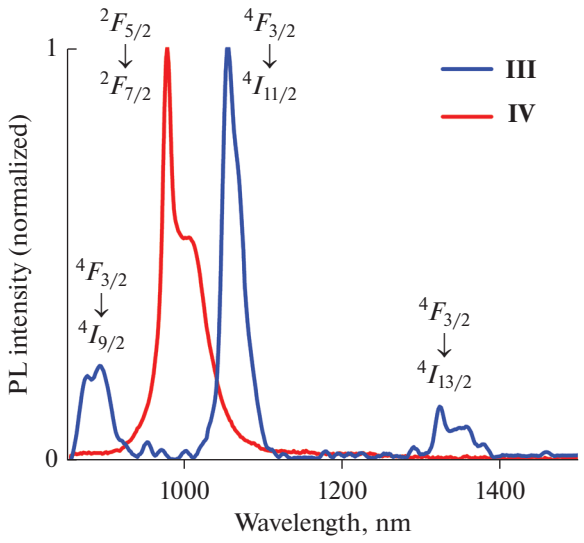

Fig. 7. PL spectra of solid samples of **III** and **IV** in the IR range at room temperature, λ_{excit} = 405 nm.

FUNDING

This study was supported by the Russian Science Foundation (grant no. 20-73-10115).

CONFLICT OF INTEREST

The authors of this work declare that they have no conflicts of interest.

REFERENCES

1. Bünzli, J.C.G., *Handb. Phys. Chem. Rare Earths*, 2016, vol. 50, p. 141.
2. Bünzli, J.C.G., *Coord. Chem. Rev.*, 2015, vols. 293–294, p. 19.
3. Bryleva, Y.A., Artem'ev, A.V., Glinskaya, L.A., et al., *New J. Chem.*, 2021, vol. 45, p. 13869.
4. Ivanova, A.A., Gontcharenko, V.E., Lunev, A.M., et al., *Inorganics*, 2022, vol. 10, p. 104.
5. Alzard, R.H., Siddig, L.A., Saleh, N., et al., *Sci. Rep.*, 2022, vol. 12, p. 1.
6. Nosov, V.G., Kupryakov, A.S., Kolesnikov, I.E., et al., *Molecules*, 2022, vol. 27, p. 5763.
7. Liu, W., Li, D., Wang, F., et al., *Opt. Mater.*, 2022, vol. 123, p. 111895.
8. Yu, X., Ryadun, A.A., Pavlov, D.I., et al., *Angew. Chem.*, 2023, p. 135, p. e202306680.
9. Wang, S., Sun, B., Su, Z., et al., *Inorg. Chem. Front.*, 2022, vol. 9, p. 3259.
10. Mínguez Espallargas, G. and Coronado, E., *Chem. Soc. Rev.*, 2018, vol. 47, p. 533.
11. Bazhina, E.S., Shmelev, M.A., Voronina, J.K., et al., *New J. Chem.*, 2023, vol. 47, p. 19251.
12. Wang, X., Wang, Y., Wang, Y., et al., *Chem. Commun.*, 2020, vol. 56, p. 233.
13. Yoon, M., Srirambalaji, R., and Kim, K., *Chem. Rev.*, 2012, vol. 112, p. 1196.
14. Getman, R.B., Bae, Y.S., Wilmer, C.E., et al., *Chem. Rev.*, 2012, vol. 112, p. 703.
15. Li, J.R., Sculley, J., and Zhou, H.C., *Chem. Rev.*, 2012, vol. 112, p. 869.
16. Furukawa, H., Cordova, K.E., O'Keeffe, M., et al., *Science*, 2013, vol. 341, p. 1230444.
17. Xia, T., Cao, W., Guan, L., et al., *Dalton Trans.*, 2022, vol. 51, p. 5426.
18. Zhou, Z., Shang, M., Yao, Z., et al., *Dye Pigment*, 2022, vol. 198, p. 110016.
19. Demakov, P.A., Sapchenko, S.A., Samsonenko, D.G., et al., *J. Struct. Chem.*, 2019, vol. 60, p. 815.

20. Songlin, Y., Dongxue, S., Kaisu, L., et al., *Dye Pigment*, 2023, vol. 220, p. 111673.
21. Belousov, Y.A., Metlin, M.T., Metlina, D.A., et al., *Polymers*, 2023, vol. 15, p. 867.
22. Ilichev, V.A., Rogozhin, A.F., Rumyantcev, R.V., et al., *Inorg. Chem.*, 2023, vol. 62, p. 12625.
23. Rogozhin, A.F., Ilichev, V.A., Fagin, A.A., et al., *New J. Chem.*, 2022, vol. 46, p. 13987.
24. Balashova, T.V., Kukinov, A.A., Pushkarev, A.P., et al., *J. Lumin.*, 2018, vol. 203, p. 286.
25. Ilichev, V.A., Rozhkov, A.V., Rumyantcev, R.V., et al., *Dalton Trans.*, 2017, vol. 46, p. 3041.
26. Shavaleev, N.M., Scopelliti, R., Gumy, F., et al., *Inorg. Chem.*, 2009, vol. 48, p. 6178.
27. Katkova, M.A., Balashova, T.V., Ilichev, V.A., et al., *Inorg. Chem.*, 2010, vol. 49, p. 5094.
28. Ilichev, V.A., Rogozhin, A.F., Belyakova, A.V., et al., *Organometallics*, 2023, vol. 42, p. 2792.
29. Hu, J.X., Karamshuk, S., Gorbaciova, J., et al., *J. Mat. Chem. C*, 2018, vol. 6, p. 7012.
30. Inbasekaran, M. and Strom, R., *The New Journal for Organic Synthesis*, 1991, vol. 449, p. 48674.
31. *Rigaku Oxford Diffraction. CrysAlis Pro Software System, version 1.171.41.122a*, Wroclaw: Rigaku Corporation, 2021.
32. Sheldrick, G.M., *Acta Crystallogr., Sect. A: Cryst. Adv.*, 2015, vol. 71, p. 3.
33. Sheldrick, G.M., *Acta Crystallogr., Sect. C: Struct. Chem.*, 2015, vol. 71, p. 3.
34. Watts, S., Peloquin, A.J., Bandara, M., et al., *Acta Crystallogr., Sect. C: Struct. Chem.*, 2022, vol. 78, p. 702.
35. Jebbari, S., Abdellatif, E.K., Ahbada, M., et al., *IUCrDATA*, 2019, vol. 4, Px191119.
36. Janiak, C., *J. Chem. Soc., Dalton Trans.*, 2000, p. 3885.
37. Shannon, R.D., *Acta Crystallogr., Sect. A: Cryst. Phys., Diffr., Theor. Gen. Crystallogr.*, 1976, vol. 2, p. 751.
38. Batsanov, S.S., *Inorg. Mater.*, 2001, vol. 37, p. 871.
39. Armstrong, D.R., Banbury, F.A., Davidson, M.G., et al., *J. Chem. Soc., Chem. Commun.*, 1992, p. 1492.
40. Kreider Mueller, A., Rong, Y., Owena, J.S., et al., *Dalton Trans.*, 2014, vol. 43, p. 10852.
41. Prasanna, M.D. and Guru Row, T.N., *Cryst. Eng.*, 2000, vol. 3, p. 135.
42. Katkova, M.A., Borisov, A.V., Fukin, G.K., et al., *Inorg. Chim. Acta*, 2006, vol. 359, p. 4289.

Translated by Z. Svitanko